

Cell Death and Neuronal Replacement during Formation of the Avian Ciliary Ganglion

Vivian M. Lee, Gregory G. Smiley, and Rae Nishi¹

Department of Cell & Developmental Biology, L-215, Oregon Health Sciences University, 3181 SW Sam Jackson Park Road, Portland, Oregon 97201

Programmed cell death is a prominent feature of embryonic development and is essential in matching the number of neurons to the target tissues that are innervated. Although a decrease in neuronal number which coincides with peripheral synaptogenesis has been well documented in the avian ciliary ganglion, it has not been clear whether cell death also occurs earlier. We observed TUNEL-positive neurons as early as stage 24, with a large peak at stage 29. This cell death at stage 29 was followed by a statistically significant ($P < 0.0001$) decrease in total neuron number at stage 31. The total number of neurons was recovered by stage 33/34. This suggested that dying neurons were replaced by new neurons. This replacement process did not involve proliferation because bromodeoxyuridine applied at stages 29 and 31 was unable to label neurons harvested at stage 33/34. The peak of cell death at stage 29 was increased 2.3-fold by removal of the optic vesicle and was reduced by 50% when chCNTF was overexpressed. Taken together, these results suggest that the regulation of neuron number in the ciliary ganglion is a dynamic process involving both cell death and neural replacement from postmitotic precursors prior to differentiation and innervation of target tissues. © 2001 Academic Press

Key Words: parasymphatic; apoptosis; Hu; TUNEL; cranial neural crest; peripheral nervous system; ciliary neurotrophic factor.

INTRODUCTION

The normal development of multicellular organisms requires cell death. Cell death is used to eliminate superfluous cells, sculpt tissues, regulate organ size, and eliminate damaged cells (reviewed in Vaux and Korsmeyer, 1999). Much of the cell death that occurs during development is highly predictable and appears to be “programmed.” For example, the development of the nematode *Caenorhabditis elegans* occurs through a precise, stereotypic pattern of cell divisions and cell deaths of embryonic cells (Ellis and Horvitz, 1986). The term “programmed cell death” was coined to describe the massive loss of intersegmental muscles during insect metamorphosis (Lockshin and Williams, 1965) and is now used to describe most cases of cell death that are actively induced by the expression of specific genes.

In the nervous system, programmed cell death is prominent throughout normal development (for review, see Nijhawan *et al.*, 2000). Cell death occurs during neurogenesis in the ventricular layer of the neural tube (Blaschke *et al.*,

1996; Homma *et al.*, 1994), and neural hypertrophy is observed when this cell death is prevented (Kuida *et al.*, 1996). In the developing spinal cord, three distinct zones of pyknotic nuclear profiles have been observed and these have been postulated to play a role in early phenotypic selection (Homma *et al.*, 1994). By far the best studied cell death coincides with synaptogenesis in postmitotic neurons (Oppenheim, 1991). After neurons have differentiated and extended axons to their targets, 40–60% of the original number are eliminated. The number of neurons that die is not preprogrammed but is affected by the target. For example, fewer neurons survive when the target of innervation is removed, and more neurons are found when extra target is added. Such studies have led to the formulation of the trophic hypothesis, which states that cell death is induced by a limiting amount of neurotrophic factor produced by the target tissues (Barde, 1989). A great deal of support for the trophic hypothesis comes from studies of nerve growth factor and its relatives, the neurotrophins.

One system in which target-dependent neuronal death can be readily studied is the avian ciliary ganglion (CG). The CG is formed by cells that migrate from the neural crest of the caudal mesencephalon and rostral metencephalon (Noden, 1975). The neural precursors withdraw from

¹ To whom correspondence should be addressed. Fax: (503) 494-4253. E-mail: nishir@ohsu.edu.

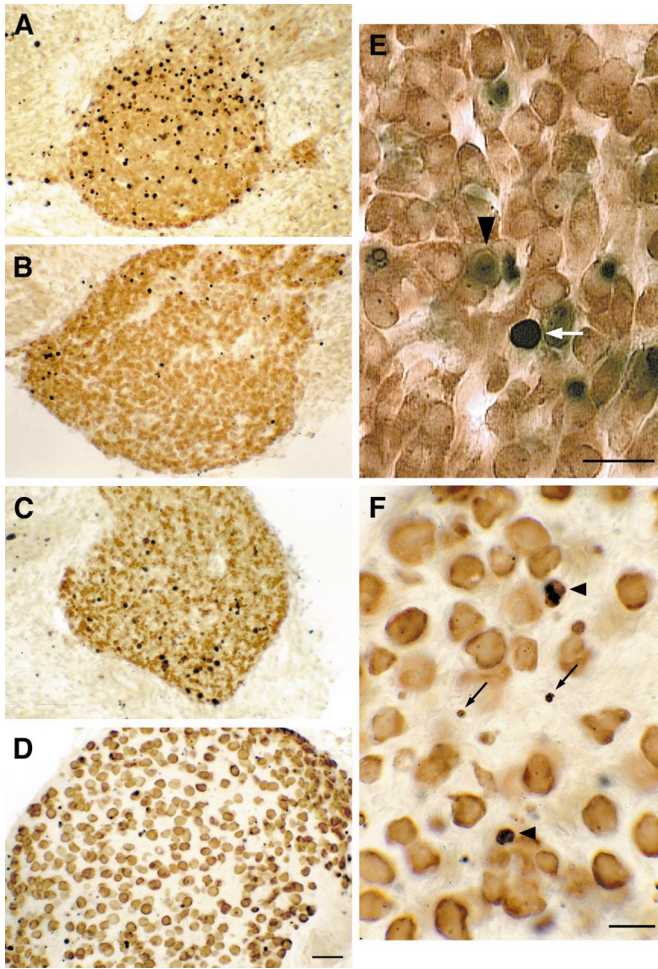


FIG. 1. Pattern of dying cells in the ciliary ganglion. CG were collected and processed for TUNEL and anti-HuC/D immunocytochemistry at various embryonic ages. TUNEL labels are black and nuclear; HuC/D immunoreactivity is brown, cytoplasmic, and neuron-specific. (A–D) Low-magnification photomicrographs of St. 29, 31, 33/34, and 38 CG that were processed for TUNEL and HuC/D immunocytochemistry. (A) At St. 29, a large number of TUNEL⁺ cells could be seen throughout the CG. (B) At St. 31, the number of dying cells was low compared to other stages (A, C, D). (C) There are more dying cells at St. 33/34 compared to St. 31 (B) but less than at St. 29 (A). (D) TUNEL⁺ nuclei of varying sizes could be seen at St. 38 CG. (E) Higher magnification of TUNEL- and HuC/D-labeled St. 29 CG showing that some TUNEL-labeled nuclei were as large as intact neuronal nuclei (white arrow) and some of them could be observed within a HuC/D-positive cytoplasm (black arrowhead). (F) Higher magnification of TUNEL- and HuC/D-labeled CG at St. 38 (E12) showing some TUNEL-labeled nuclei close to other neurons with nuclei roughly the same size as a neuron (arrowheads). There were also a number of TUNEL-labeled nuclei that were much smaller and located in areas that were devoid of neurons (small arrows). Scale bars A–D, 50 μ m; E and F, 20 μ m.

the mitotic cycle at E5.5 (D'Amico-Martel, 1982) and the CG is numerically complete by St. 31 (Landmesser and Pilar, 1974b). Two types of neurons differentiate within the

CG, ciliary and choroid (Marwitt *et al.*, 1971). Both types of CG neurons innervate tissues in the eye, which can be readily removed prior to the formation of the CG. Between St. 35 and St. 40 (E9 to E14), the number of neurons in the CG is reduced by 50% (Landmesser and Pilar, 1974b). This reduction in number coincides with peripheral synaptogenesis, changes in neuronal ion channels, induction of choline acetyltransferase activity, expression of somatostatin in choroid neurons, and gliogenesis (Dryer, 1994; Nishi, 1994). When the optic cup is ablated more than 90% of the neurons die (Landmesser and Pilar, 1974b). In contrast, when an extra eye is transplanted, thereby making more target tissue available, fewer CG neurons die (Narayanan and Narayanan, 1978). Furthermore, when a portion of the ciliary and iris muscle is denervated by cutting one branch of the ciliary nerve, the resulting free synaptic space is taken over by neighboring ciliary neurons, resulting in a higher degree of survival (Pilar *et al.*, 1980). Neurotrophic factors that support CG neuron survival in cell culture are ciliary neurotrophic factor (CNTF) and glial cell line-derived neurotrophic factor (GDNF). Chicken CNTF is expressed in target tissues of ciliary ganglion neurons during and after the period of cell death (Finn and Nishi, 1996), and CNTF also rescues CG neurons from cell death when overexpressed in the eye (Finn *et al.*, 1998).

In considering the possible mechanisms of target-

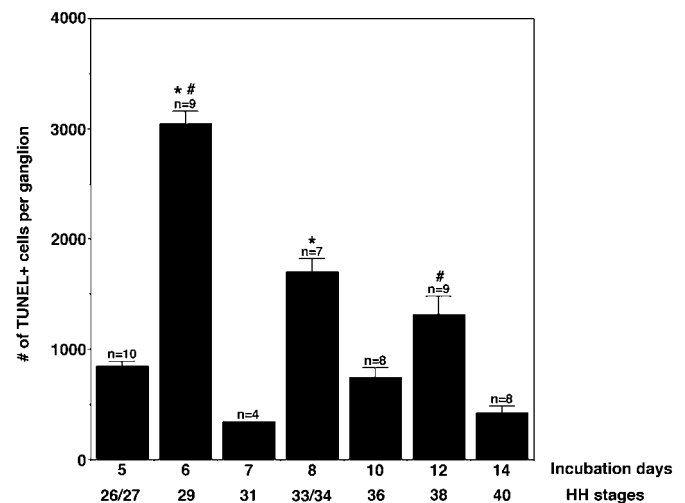


FIG. 2. Quantification of TUNEL-labeled cells in the developing CG. The total number of TUNEL⁺ cells in St. 26–40 CG were counted using design-based stereology and their values are represented as histograms (means \pm SEM). Cell death could be seen throughout CG development. The largest peak of TUNEL⁺ cells was observed at St. 29. A second peak appeared at St. 33/34 (value between St. 29 and St. 33/34; * P < 0.0001, Student's t test). At St. 31, there were many fewer dying cells compared to St. 29 and St. 33/34. At St. 38 there was another wave of dying cells, but the value was smaller compared to St. 29 (# P < 0.0001, Student's t test). The number of CG counted for each time point (n) is listed on top of each bar; y error bars, SEM.

dependent cell death we sought to determine the timing of commitment to death with the disappearance of viable neurons. Because previous studies in the CG have usually monitored changes in total neuron number, we focused on identifying dying neurons by using an *in situ* labeling method for fragmented DNA. To our surprise, we discovered that neurons in the CG were dying at much earlier stages than expected—while neuronal cell loss occurred between St. 35 and St. 40, we observed neurons dying as early as St. 24, with a large peak representing 13% of the total at St. 29. The peak of cell death was followed by a decrement in total neuron number at St. 31, which recovered by St. 33/34 to the number found at St. 29. The peak of cell death observed at St. 29 could be modified by target extirpation as well as overexpression of chicken (ch) CNTF.

MATERIALS AND METHODS

Tissue Preparation and Islet-1 Immunocytochemistry for Stereology

White Leghorn × New Hampshire Red (Animal Sciences Department, Oregon State University, Corvallis, OR) or pathogen-free

White Leghorn (SPAFAS, used for retroviral studies) fertile eggs were incubated at 38°C in Roll-Ex egg incubators (Lyon Electric Co., Chula Vista, CA). Chick embryos were staged according to Hamburger and Hamilton (1951) and ciliary ganglia dissected as previously described (Nishi, 1996). CG were immediately fixed in 4% paraformaldehyde in phosphate-buffered saline (PBS; 150 mM NaCl, 20 mM sodium phosphate, pH 7.4) for 2 to 3 h at room temperature (RT) or overnight at 4°C. After being rinsed three times in PBS, tissues were allowed to equilibrate in 30% sucrose in PBS overnight at 4°C. Serial sections were cut at 30 μm on a Leica Jung cryostat at -25°C and collected on gelatin/poly-L-lysine-subbed slides. Slides were air dried for 15 min and postfixed for 15 min in 4% paraformaldehyde vapors followed by complete immersion for 15–30 min. Slides were washed three times in PBS and incubated overnight at 4°C in blocking solution (2% (w/v) bovine serum albumin (BSA), 2% (v/v) normal goat serum, 0.5% (v/v) Triton X-100, and 0.2% (w/v) sodium azide in PBS). Sections were then incubated with anti-islet-1 (1:250 hybridoma supernatant, clone 39.405, which recognizes both islet-1 and islet-2; Developmental Studies Hybridoma Bank, University of Iowa) in blocking solution overnight at 4°C. Following three washes with PBS and 0.5% (v/v) Triton X-100 (PBST) and inactivation of endogenous peroxidase with 0.5% H₂O₂, slides were incubated for 1.5 h at room temperature with a biotinylated goat anti-mouse antibody (1:500; Vector Laboratories), followed by three washes with PBST. Finally,

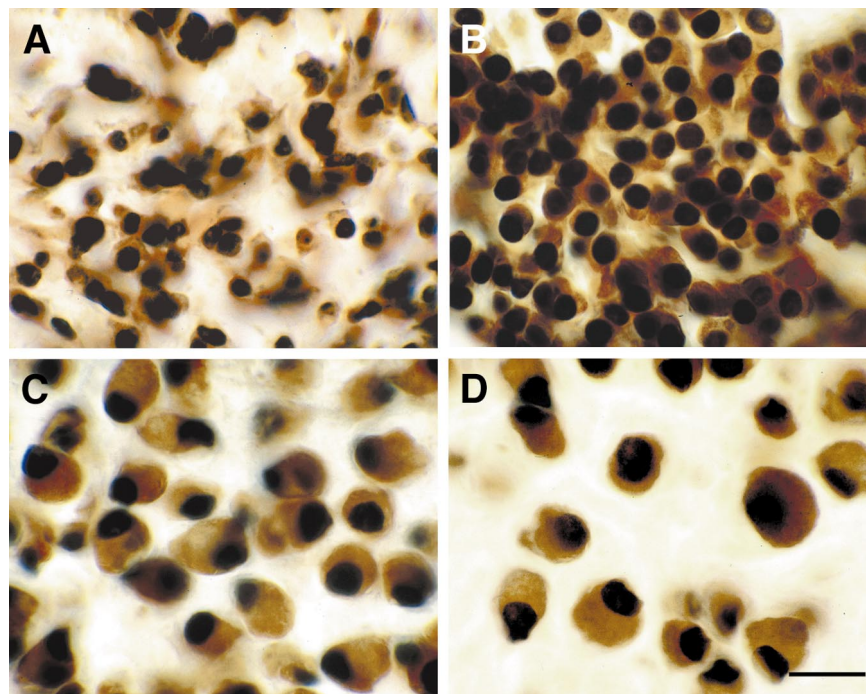


FIG. 3. CG neurons express islet-1 throughout development. CG neurons expressed both islet-1 and HuC/D as early as St. 24 and persisted until St. 40. CG sections were processed for anti-islet-1 (black) and anti-HuC/D (brown) immunoreactivity. Anti-islet-1 immunoreactivity was nuclear while anti-HuC/D was cytoplasmic. At all stages examined virtually all of the islet-1-positive nuclei were located within cell bodies expressing HuC/D immunoreactivity. (A) At St. 24, anti-islet-1 and HuC/D identified neurons as soon as they commenced differentiation. (B) At St. 29, CG neurons were tightly packed together, but the dark, nuclear staining of anti-islet-1 allowed easy identification and greatly facilitated counting individual neurons. (C) St. 36 CG. (D) St. 38 CG. After St. 36, the volume of CG increased, with a corresponding increase in the size and separation of islet-1⁺ neurons (compare D with B). A–D were taken at the same magnification, scale bar, 20 μm.

sections were incubated for 1.5 h at RT in the Vectastain ABC-HRP solution (1:500; Vector Laboratories). Islet-1 immunoreactivity was visualized by nickel/cobalt enhanced diaminobenzidine (NiDAB) solution (0.5 mg/ml DAB (Sigma), 0.1% NiCl₂, 0.1% CoCl₂, and 0.01% H₂O₂ in PBS). After color development, slides were rinsed three times in PBS and incubated in blocking solution for an hour at RT. Sections were then incubated in anti-HuC/D (1:250; Molecular Probes) in blocking buffer overnight at 4°C. Slides were treated with secondary antibody and ABC-HRP as described above. Anti-HuC/D immunoreactivity was detected by reaction with 0.5 mg/ml DAB without nickel/cobalt enhancement.

Detection of Dying Cells with TUNEL

CG were fixed in 4% paraformaldehyde containing 1 mM EDTA to inhibit DNase activity. After fixation, slides were blocked in 2% BSA, 2% sheep serum in PBST overnight at 4°C. TUNEL assays were performed using the In Situ Cell Death Detection, POD kit (Roche Biochemicals), which incorporates fluorescein isothiocyanate (FITC)-labeled nucleotides into the free 3'OH ends of DNA and amplifies the labeled DNA with an antibody against FITC that is conjugated to horseradish peroxidase (POD). The following modifications were made to the manufacturer's protocol: (1) the nucleotide labeling mix was diluted 1:1 and the reaction was run for 3 h; (2) the anti-fluorescein POD was diluted 1:5 and incubated for 2.5–3 h; (3) TUNEL labeling was visualized by incubating tissue sections in NiDAB solution. All sections were then processed for anti-HuC/D immunocytochemistry as described above.

Cell Counting Using Design-Based Stereology

We counted islet-1- and TUNEL-positive cells with design-based stereology using an optical fractionator probe (West *et al.*, 1991). In order to use this technique to its full efficiency, tissue collapse during processing had to be minimized. We mounted 6–10 CG together and cut 30- μ m serial cryostat sections which were collected on slides and processed for immunohistochemistry for islet-1 and HuC/D. When we measured our sections after staining and mounting, their thickness was consistently 26–28 μ m, demonstrating that our processing method could preserve tissue integrity. In addition, islet-1⁺ nuclei were observed throughout the entire z axis of the sections, confirming that our immunocytochemical reagents penetrated the entire thickness of the tissue.

Stereology software (Stereo Investigator, Microbrightfield) was used in conjunction with a Nikon Optiphot microscope with an x, y, z stage drive and a position transducer. Spacing between sampling sites (grid size) was set such that 10–12 sampling sites per section were counted, according to manufacturer's instructions. Each sampling site was adjusted to contain 0–5 counting objects so that 100–300 cells were counted for each ganglion. Because CG increased in volume as the embryo developed (see Results), grid sizes were adjusted in order to normalize the sampling criteria across the embryonic ages. Counting frame and grid size were determined for each age by counting each section at least three times with or without the same sampling sites, conditions that yielded cell counts that were within 5% of error were chosen for subsequent quantification. In addition, an upper guard zone of 4 μ m and a lower guard zone of 7 μ m were used to restrict counting to the volume of tissue sections that was devoid of cutting artifacts. To establish the reliability of our cell counting method, we counted the same sections across various developmental ages at least three times using the same sampling sites, then repeated with different sampling sites. The margin of error of these counts was within 5%.

Bromodeoxyuridine (BrdU) Treatment and Immunocytochemistry

BrdU (25 μ g; Roche Biochemicals) was injected into the amnion of embryos between St. 24 and St. 31. Treated embryos were collected at St. 33/34 and processed as described above. Cryostat sections (25 μ m) were cut and treated with 50 μ g/ml DNase I (Roche) for 30 min at 37°C after fixation followed by three rinses in PBS + 1 mM EDTA and once in PBS. Slides were incubated in anti-HuC/D (1:250) and anti-BrdU (1:500; Harlan SeraLab) together overnight at 4°C. Anti-HuC/D and anti-BrdU immunoreactivities were visualized by incubating sections in Alexa 488-conjugated goat anti-mouse IgG and Cy3-conjugated donkey anti-rat IgG (Jackson ImmunoResearch), respectively. Fluorescent images were acquired using a Leica inverted microscope equipped with a digital camera.

HuA and HuC/D Immunohistochemistry

St. 29 CG were collected and fixed as described (see Tissue Preparation and Islet-1 Immunocytochemistry for Stereology). Ten-micrometer cryostat sections were cut and postfixed in 4% paraformaldehyde for 10–20 min at RT. Slides were incubated in anti-HuA (gift from Dr. Marusich and Dr. Weston, University of Oregon) and anti-HuC/D together overnight at 4°C. Anti-HuA immunoreactivity was visualized by using an Alexa 488-conjugated goat anti-mouse IgG1 and anti-HuC/D by an Alexa 568-conjugated goat anti-mouse IgG2b. Fluorescent images were taken on a Bio-Rad 1024 laser scanning confocal microscope and optical sections were collected at 1- μ m intervals.

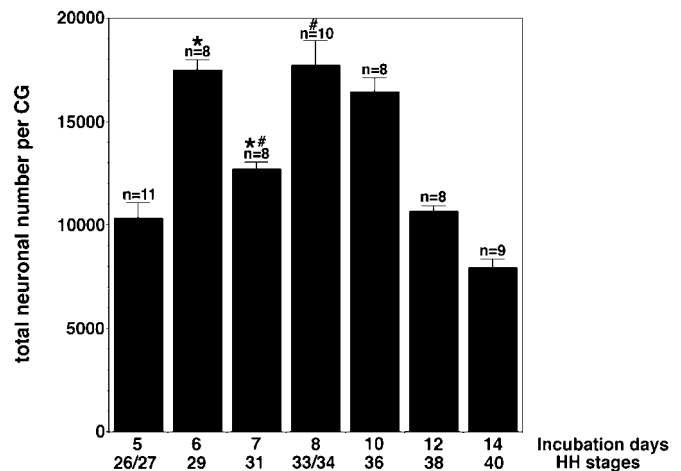


FIG. 4. Quantification of neuronal number in the developing CG using anti-islet-1 as a neuron-specific marker. Total number of islet-1-positive neurons between St. 26 and St. 40 were counted using design-based stereology. The maximum number of neurons was observed at St. 29 (17,502 \pm 462) followed by a decrease at St. 31 (12,701 \pm 331; value between St. 29 and St. 31; **P* < 0.0001, Student's *t* test); however, by St. 33/34 the neuronal number returned to a level comparable to St. 29 (17,714 \pm 1193; value between St. 31 and St. 33/34; #*P* < 0.001, Student's *t* test). Between St. 33/34 and St. 40 the number of neurons decreased by 55%. The number of CG counted for each time point (n) is listed on top of each bar; y error bars, SEM.

Optic Vesicle Ablation

Surgeries were performed on St. 11–13 embryos as previously described (Landmesser and Pilar, 1974a). Briefly, embryos were exposed by windowing the eggs and neutral red was used to visualize the embryos. Sharpened tungsten needles were used to remove one of the optic vesicles in each embryo; the eggs were sealed with scotch tape and returned to the incubator until St. 29.

Production of Stable Virus Producer Cells and High-Titer Viral Inoculum

Stable virus producer cells were generated by calcium phosphate transfection with pRCASBP(A)-chCNTF (Finn *et al.*, 1998) and pRCASBP(A)-GFP (kindly provided by C. Cepko) as previously described (Morgan and Fekete, 1996) with the exception that the continuous chicken fibroblast cell line DF-1 (Himly *et al.*, 1998) was used rather than primary chicken embryo fibroblasts. Infection by RCASBP(A) and transgene expression (chCNTF) in DF-1 cells were verified by p27gag and chCNTF immunocytochemistry, respectively. The DF-1 cells continued to show complete viral infection with no loss in transgene expression after 20+ passages. Culture supernatants containing virus were concentrated approximately 100-fold by ultracentrifugation at 70,000g. The concentrated viral stocks used throughout these experiments were from the same lot and had titers of approximately 4.3×10^8 infectious units (IU)/ml (RCASBP(A)-GFP) and 2.0×10^8 IU/ml (RCASBP(A)-chCNTF). Concentrated virus (250–350 nl) was injected into the lumen of the developing mesencephalon in St. 8–10 embryos using a Nanoject II positive displacement microinjector (Drummond) mounted to a micromanipulator (Marhauser Model MM33). Embryos were returned to incubators until they were harvested at St. 29.

Cell Culture and Anti-chCNTF Receptor α (Anti-chCNTFR α) Immunocytochemistry

CG from St. 29 embryos were dissociated and plated on polylysine-laminin-coated tissue culture coverslips (Fisher) as previously described (Nishi, 1996) with the modification that the incubation in trypsin was shortened to 10 min. Recombinant [his]6-chCNTFy (Finn *et al.*, 1998) was used at 10 ng/ml. Cultures were assessed for neuronal survival and photographed 24 h after plating. Live St. 29 cultures were incubated in a rabbit anti-chCNTFR α antibody at 37°C for 30–45 min. After fixation in 4% paraformaldehyde, cultures were rinsed in PBS three times and blocked in PBS with 2% BSA and 2% normal goat serum for an hour at RT. CG cultures were then incubated in anti-HuC/D overnight at 4°C. Anti-chCNTFR α was visualized by using an Alexa 488-conjugated goat anti-rabbit secondary antibody (Molecular Probes) and anti-HuC/D was visualized by a Rhodamine Red-X-conjugated goat anti-mouse secondary antibody (Jackson ImmunoResearch).

In Situ Hybridization

A 745-bp chCNTFR α fragment was cloned into the *Nco*I site of pGEM5z (Promega) and antisense and sense digoxigenin-labeled riboprobes were generated using the MegaScript SP6 and T7 kits (Ambion). Hybridization was carried out at 65°C followed by washes at the same temperature. Tissue sections were then incubated in alkaline phosphatase-conjugated anti-digoxigenin (Roche) overnight at 4°C. *In situ* hybridization product was visualized using a NBT/BCIP substrate.

RESULTS

Cell Death of CG Neurons Occurs during Early Embryonic Development

Dying cells identified by TUNEL, which labeled fragmented DNA, could be seen throughout development in the CG (Fig. 1). TUNEL⁺ nuclei were observed as early as St. 24. To test whether the labeled cells were neuronal, we also stained the same tissue sections with an antibody against HuC/D, a RNA binding protein that is expressed only in neurons (Marusich *et al.*, 1994; Wakamatsu and Weston, 1997). Many of the TUNEL-labeled nuclei between St. 26 and St. 33/34 were surrounded by HuC/D⁺ cytoplasm (Figs. 1A–1C and 1E). At these early stages of CG development, we observed many TUNEL⁺ nuclei that were comparable in diameter to the nuclei of healthy neurons, indicating that dying neurons could be detected prior to the formation of a pyknotic nucleus (Fig. 1E).

We quantified the total number of TUNEL⁺ cells between St. 26 and St. 40 using design-based stereology (Fig. 2). The largest peak of cell death was seen at St. 29 (3043 ± 113 ($n = 9$); Figs. 1A and 2). The large peak at St. 29 was followed by another one at St. 33/34 (1703 ± 120 ($n = 7$)) and a third, smaller peak at St. 38 (1319 ± 165 ($n = 9$)). Each peak of TUNEL⁺ nuclei was followed by a significant decrease the following day (Figs. 1A–1C and 2), suggesting that cells committed to dying were cleared within 24 h. In addition, the large peak of cell death at St. 29 was followed by a decrease in total neuron number at St. 31 (compare Figs. 2 and 4). Thus, the TUNEL reaction most likely labeled cells committed to dying, rather than cells in the process of DNA repair. Many TUNEL⁺ nuclei were associated with HuC/D⁺ cytoplasm between St. 24 and St. 34 (Fig. 1D and data not shown), indicating that the majority of the dying cells at early stages were neurons. After St. 36, some TUNEL-labeled cells appeared neuronal but were small and often not associated with HuC/D immunoreactivity, suggesting that they represented apoptotic nuclei contributed by both neurons and nonneuronal cells in the CG (Fig. 1F). At St. 40, there were relatively fewer TUNEL-labeled nuclei (422 ± 65 , $n = 8$; Fig. 2) compared to St. 38, consistent with the observation that developmental cell death in CG ceases by St. 40.

A Reexamination of the CG Using Islet-1 Immunoreactivity Confirms That Cell Number Declines between St. 33/34 and St. 40

To determine when cell death occurred relative to a reduction in overall survival, we reexamined neuronal number in the CG. Accordingly, we characterized the staining pattern of a transcription factor, islet-1, which had previously been shown to identify motor neurons (Ericson *et al.*, 1992; Tsuchida *et al.*, 1994) and other peripheral neurons (Avivi and Goldstein, 1999). As early as St. 24 (Fig. 3A) we observed islet-1 immunoreactivity in the CG. This suggested that CG neurons expressed islet-1 very early, perhaps as soon as the mesencephalic neural crest cells

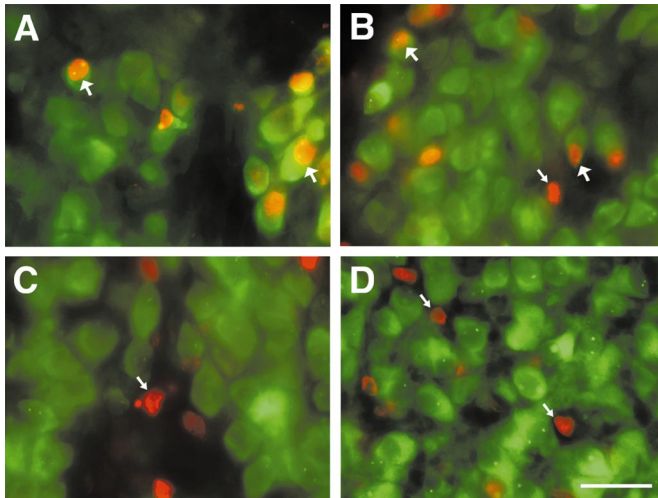


FIG. 5. No CG neurons were generated by proliferation after St. 29. Chick embryos were treated with BrdU at St. 24 (A), St. 26/27 (B), St. 29 (C), and St. 31 (D) and CG harvested at St. 33/34. (A and B) BrdU-positive nuclei (red) could be seen within HuC/D-positive neurons (green) when embryos were pulsed with BrdU at St. 24 and St. 26/27 (A and B, big white arrows). (A) When BrdU was added onto St. 24 embryos, BrdU⁺ neurons (HuC/D⁺) could be observed at St. 33/34 (big white arrows). (B) When BrdU was added to St. 26/27 embryos, BrdU⁺/HuC/D⁺ neurons (big white arrows) as well as BrdU⁺-only nuclei (small white arrow) could be observed, suggesting that some neurons and nonneuronal cells were dividing at that age. (C and D) When we pulsed embryos with BrdU at or after St. 29, no BrdU⁺/HuC/D⁺ neurons could be labeled. Small arrows in C and D pointed to BrdU⁺-only nuclei, suggesting that no CG neurons underwent cell division after St. 29. (C) BrdU added to St. 29 embryos yielded no BrdU⁺ neurons at St. 33/34. (D) BrdU applied at St. 31 also did not result in BrdU⁺ neurons. Red, BrdU; green, HuC/D; scale bar, 20 μ m.

commenced differentiating as CG neurons. When we examined other embryonic ages, we found that virtually all CG neurons coexpressed *islet-1* and HuC/D from St. 24 to 40, confirming that *islet-1* is a valid marker for all CG neurons. In addition, the nuclear localization of *islet-1* greatly facilitated the counting of CG neurons, especially at early stages (St. 26–34; Figs. 3A and 3B and data not shown) when neuronal profiles were small and the ganglia were tightly packed with both neuronal and nonneuronal nuclei. At later ages, the volume of the CG expanded considerably and neurons were spaced further apart (compare Figs. 3A and 3B to 3C and 3D), presumably because of the proliferation and differentiation of the nonneuronal cells in the CG.

We quantified the total number of CG neurons from staged embryos (Hamburger and Hamilton, 1951) between St. 26 and St. 40 (Fig. 4). The number of neurons in the CG increased from $10,344 \pm 731$ ($n = 11$) at St. 26/27 (E5) to $17,502 \pm 462$ ($n = 8$) at St. 29. This increase presumably represented the differentiation of neurons from neural crest cell committed to the neural lineage (D'Amico-Martel, 1982). The peak in neuronal number at St. 29 was followed

by a decrease in neuronal number to $12,701 \pm 331$ ($n = 8$) at St. 31, but the number returned to $17,714 \pm 1193$ ($n = 10$) by St. 33/34. The lowered number of neurons at St. 31 was statistically significant from the number observed at St. 29 and St. 33/34 by using the Student *t* test ($P < 0.0001$). In confirmation of previous observations (Finn *et al.*, 1998; Furber *et al.*, 1987; Landmesser and Pilar, 1974b), we saw a 50% reduction in the number of neurons between St. 33/34 and St. 40.

Dying Neurons Are Replaced by Postmitotic Precursors

The cell death we observed at St. 29 together with the statistically significant reduction in total neuron number from St. 29 to St. 31, which recovered by St. 33/34, suggested that dying neurons could be replaced by newly differentiated cells. Previous studies by several groups have shown that CG neurons were not labeled if [³H]thymidine is injected into embryos after E5.5 (D'Amico-Martel, 1982; Rohrer and Thoenen, 1987). It was possible that some newly generated neurons were not detected due to the limited ability of [³H]thymidine to penetrate photographic emulsion; thus, we tested whether dying neurons were replaced from a proliferating neural precursor by applying BrdU to chick embryos at various stages of development and examining St. 33/34 CG for colocalization of BrdU with HuC/D immunoreactivity. When BrdU was applied at St. 24, many neuronal nuclei were BrdU positive (Fig. 5A);

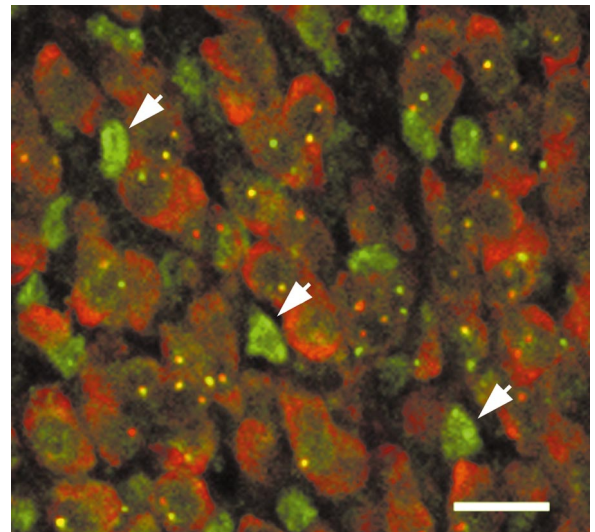


FIG. 6. St. 29 CG contains a subpopulation of cells that express only HuA, a marker of undifferentiated cells. St. 29 chick CG were fixed, cryostat sectioned, and double stained for HuA (green) and HuC/D (red). Sections were imaged by confocal microscopy. While all differentiated neurons expressed both HuA and HuC/D antigens, many singly labeled HuA cells could be observed in the ganglion (white arrows). These HuA⁺, HuC/D⁻ cells may be the cells that replace CG neurons that die at St. 29. Scale bar, 10 μ m.

application of BrdU at St. 26/27 resulted in a mixture of labeling in neurons and nonneuronal cells (Fig. 5B). In contrast, when BrdU was injected at St. 29 or St. 31, many small, nonneuronal nuclei could be seen labeled (Figs. 5C and 5D), but none of the BrdU immunoreactivity was colocalized with HuC/D immunoreactivity. Thus, the neurons that are formed between St. 31 and St. 33/34 do not arise from a proliferating cell population.

As a first step toward identifying the precursor population from which the CG neurons are generated, we double-stained St. 29 CG with antibodies against HuA and HuC/D. Previous studies have shown that HuA is expressed in uncommitted neural crest cells and differentiating neurons, but not in glia of the developing avian dorsal root ganglion (Wakamatsu and Weston, 1997). Figure 6 shows that a subpopulation of the nonneuronal cells in the CG express HuA, while neurons express both HuA and HuC/D, as previously reported. Interestingly, the $\text{HuA}^+/\text{HuC/D}^-$ cells are often adjacent to neurons, suggesting that direct cell/cell interactions may regulate the replacement process. The spaces lacking immunoreactivity are filled with nuclei, presumably of glial cells or glial precursors (data not shown).

Cell Death at St. 29 Is Increased by Ablation of the Optic Vesicle and Reduced by *chCNTF*

In order to test whether target deprivation caused an increase in CG neurons dying at St. 29, we ablated the developing optic vesicle at St. 11–13 and counted the number of TUNEL⁺ neurons at St. 29. Operated embryos developed normally with the exception that little or no eye formed on one side. CG that were processed looked normal and could be identified in the tissue by HuC/D immunoreactivity. We found that there were 2.3-fold more dying cells on the operated side compared to the contralateral side (Fig. 7). TUNEL⁺ nuclei on the operated side were often found associated with HuC/D⁺ cytoplasm, indicating that the additional dying cells were neuronal.

We next asked if the cell death at St. 29 could be modified by availability of trophic factor. We have previously purified and cloned a chicken ciliary neurotrophic factor (Leung *et al.*, 1992). St. 29 CG neurons expressed *chCNTFR α* *in vitro* (Figs. 8A and 8B) and *in vivo* (Figs. 8C and 8D). We then tested whether *chCNTF* could support the survival of St. 29 CG in cell culture. In the absence of *chCNTF*, all St. 29 neurons were dead 24 h after plating, but when recombinant *chCNTF* (10 ng/ml) was added, many neurons survived and they appeared phase bright and healthy (Figs. 8E and 8F). These neurons were identified by their morphology as well as immunoreactivity for the neuron-specific markers HuC/D and *islet-1* (Fig. 7C and data not shown).

We overexpressed *chCNTF* in chick embryos by using the replication-competent retroviral vector RCASBP(A). Control embryos received injections of RCASBP(A) encoding green fluorescent protein (GFP). We then harvested CG at St. 29 and quantified the TUNEL⁺ cells. RCASBP(A)-*chCNTF*-infected embryos had a 50% decrease in the num-

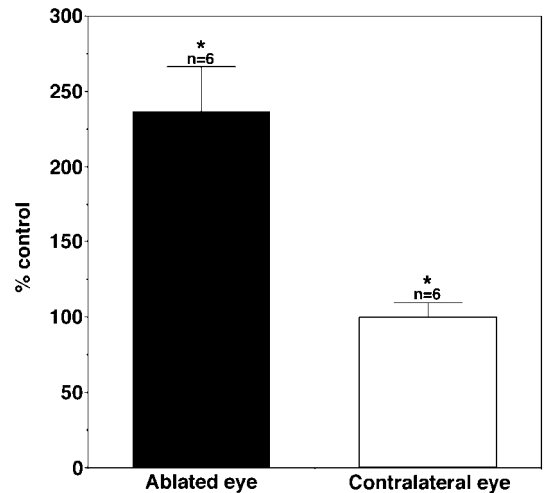


FIG. 7. Eye ablation exacerbated cell death at St. 29. Optic vesicles were removed from one eye of E2 (St. 11–13) chick embryos and the other side was left unperturbed as a control. Embryos were collected at St. 29 and their CG processed for the TUNEL assay and anti-HuC/D immunocytochemistry. The total number of TUNEL⁺ cells was counted in CG from ablated eyes and contralateral controls. The number of TUNEL⁺ cells in the ablated eye was represented as a percentage of controls. There were 2.3-fold more dying cells in the ablated side compared to the control side ($*P < 0.001$, Student's *t* test). The number of CG counted for each time point (*n*) is listed on top of each bar; *y* error bars, SEM.

ber of TUNEL⁺ cells compared to the RCASBP(A)-GFP controls (Fig. 9).

DISCUSSION

Our studies reveal new and unexpected data on the regulation of neuron number in the avian ciliary ganglion. First, we have discovered that there are significant numbers of dying neurons in the CG at St. 29, several days prior to the period of time that an actual decrement in cell number had been previously described (Furber *et al.*, 1987; Landmesser and Pilar, 1974b). Second, while there is a transient decrease in neuron number at St. 31 following the large amount of cell death at St. 29, neuron number recovers by St. 33/34, suggesting that there is a homeostatic mechanism regulating cell number in the CG. Third, the large amount of cell death at St. 29 is increased if the optic vesicle is removed and decreased by the overexpression of *chCNTF*, a trophic molecule for CG neurons.

The peak of cell death that we observed in the CG did not coincide with the greatest period of neuronal cell loss nor with functional innervation of CG targets. This differs significantly from observations in other peripheral neurons. In spinal ganglia, the number of pyknotic nuclei peaked between St. 26 and 29, which coincides with functional innervation of the limb muscle by proprioceptors located in

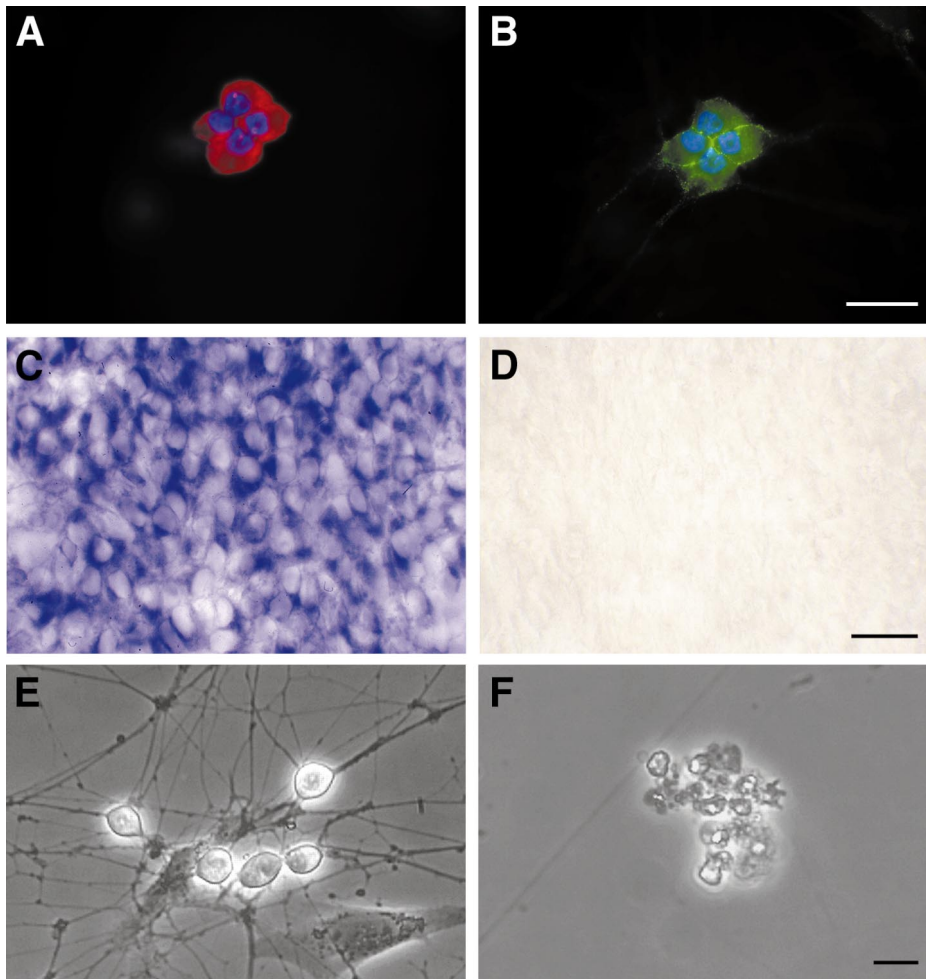


FIG. 8. St. 29 CG neurons express CNTFR α and are dependent upon CNTF for survival in cell culture. St. 29 CG neurons expressed chCNTFR α *in vitro*. (A) CG neurons identified by HuC/D immunoreactivity (red). (B) Same field of view showing neurons expressing chCNTFR α immunoreactivity (green). Transcripts for chCNTF receptor α could be observed *in vivo* by *in situ* hybridization with digoxigenin-labeled riboprobe for chCNTFR α . (C) Hybridization with the antisense probe yielded cytoplasmic staining in St. 29 CG neurons. (D) No signal was obtained when sense probe was used in the hybridization. Expression of chCNTFR α is functional—when St. 29 cultures were seeded with (E) or without (F) 10 ng/ml recombinant chCNTF, neuronal survival was supported. In CG cultures in which chCNTF was omitted all neurons were dead the following day. Scale bar in A and B, 20 μ m; scale bar in C and D, 20 μ m; scale bar in E and F, 50 μ m.

the ventrolateral region (Hamburger and Levi-Montalcini, 1949). A similar coincidence in the peak of neural degeneration with innervation of muscle has been observed in spinal cord motor neurons (Chu-Wang and Oppenheim, 1978). In part, our ability to detect cell death in the CG prior to peripheral synaptogenesis may have been due to the greater sensitivity of the TUNEL method; however, our quantification clearly shows that cell death in the CG is highest at this earlier time (St. 29). It may be possible that degenerating cell bodies persist slightly longer at St. 29, leading to a larger number that are counted; but our quantification also shows that the peaks of TUNEL labeling are followed by significant decreases in the number of

TUNEL-labeled cells within 24 h, suggesting that changes in clearance rate must be relatively subtle.

The peak of CG cell death at St. 29 also does not coincide with a period of rapid proliferation and neurogenesis, as it does in the developing central nervous system (CNS). In the CNS, an amplified TUNEL method, ISEL+, revealed a startlingly high number of dying cells during early neurogenesis (Blaschke *et al.*, 1996, 1998). As a consequence, it was estimated that >70% of the neurons generated in the neural tube could be undergoing cell death during differentiation. Although this observation remains controversial, subsequent studies of transgenic mice lacking genes encoding caspases-3 or -9 have shown that morphological devel-

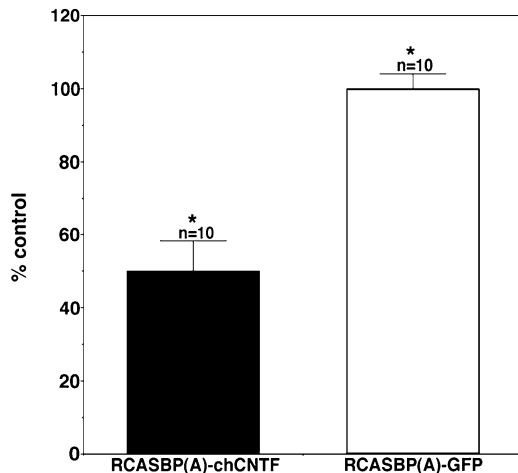


FIG. 9. Overexpression of chCNTF reduced cell death at St. 29. Retroviruses were injected into the neural tube at stage 8–9 in chick embryos. CG were harvested and processed for TUNEL and anti-Hu immunocytochemistry at St. 29. Total numbers of TUNEL⁺ cells in the CG from RCASBP(A)-chCNTF- and RCASBP(A)-GFP-injected embryos were quantified and are represented as percentage control in the histogram. The number of dying cells at St. 29 decreased by about 50% in embryos in which chCNTF was overexpressed compared to the GFP-infected controls ($*P < 0.0001$, Student's *t* test). The number of CG counted (*n*) is listed on top of each column; error bars, SEM.

opment of the CNS is disrupted by a marked hyperplasia (Kuida *et al.*, 1996, 1998). In contrast, the cell death we observe is highest after all CG neurons have undergone their last cell division, as we have confirmed with our BrdU labeling (D'Amico-Martel, 1982; Rohrer and Thoenen, 1987). In dorsal root ganglia (Hamburger and Levi-Montalcini, 1949), as well as in sympathetic ganglia, proliferation and differentiation of neuroblasts are concurrent with target-dependent cell death. This differs significantly with our observations in a parasympathetic ganglion, as well as with observations in spinal cord motor neurons.

Our data suggest a homeostatic replacement of dying neurons from postmitotic precursors. The large amount of cell death at St. 29 was followed by a significant decrease in total neuron number at St. 31, which rebounded at St. 33/34 to the total neuron number observed at St. 29. Similar observations of homeostasis in final ganglion size were reported in previous studies that manipulated neural crest cell number. For example, when an excess of neural crest cells are introduced by injection (Bronner-Fraser and Cohen, 1980) or induced by overexpressing Noelin-1 (Barembaum *et al.*, 2000), the overall range and size of neural crest derivatives are unchanged. A likely source of the postmitotic precursors are cells from the St. 29 CG that express both neuronal and nonneuronal markers (Rohrer and Sommer, 1983). Another possibility is that the CG neurons are replaced by multipotent stem cells (Shah and Anderson, 1997) or undifferentiated precursors that are quiescent at St.

29. Intriguingly, a subpopulation of nonneuronal cells at St. 29 expresses HuA. In previous studies, Wakamatsu and Weston (1997) showed that HuA was expressed at high levels in undifferentiated cells of the embryonic avian dorsal root ganglion, but not expressed in glia. Once cells commenced differentiation into neurons by upregulating HuC/D, HuA was also expressed. Thus, the HuA immunoreactivity in the nonneuronal (lacking expression of HuC/D) population of the St. 29 CG may represent cells that have the capacity to replace dying neurons. Regardless of identity, the number of replacement cells is apparently limited because dying cells outnumber replacement cells between St. 34 and St. 40, resulting in a net decrease of neurons in the CG. This is reminiscent of the restrictions in plasticity of nonneuronal crest cells in the CG observed in backtransplant experiments (Dupin, 1984; Sechrist *et al.*, 1998).

If neurons are dying at St. 29, several days before target tissues have differentiated and functional synapses have been established, then what causes this early phase of cell death? One possibility is that neural crest derivatives that migrate to the wrong location may be induced to die by the local environment, as suggested for neurogenic precursors that aberrantly migrate along the lateral pathway normally occupied by melanocytes (Wakamatsu *et al.*, 1998). We think this is unlikely because many TUNEL⁺ nuclei at St. 26/27 are found in HuC/D⁺ cells, indicating that neural differentiation has commenced, an appropriate fate for the crest destined to become the CG. Another possibility is that neurogenic precursors that differentiate into an inappropriate subtype of neuron are eliminated. For example, if cranial neural crest cells differentiate as sensory or sympathetic neurons instead of parasympathetic neurons, they may die because they lack an appropriate neurotrophic factor. This is an interesting possibility that can be tested when transcription factors that distinguish between parasympathetic and sympathetic neurons are identified. Islet-1, the marker we used to identify neurons in the CG, is also expressed in sensory and sympathetic ganglia (Avivi and Goldstein, 1999). In preliminary studies, we find that CG neurons express phox-2, a transcription factor once thought to be selective for sympathetic neurons. A final possibility is that choroid or ciliary neurons that have failed to project axons through the appropriate nerves at St. 29 die. However, there is no independent early marker for the choroid or ciliary subpopulations at St. 29; thus, there is no way to determine by retrograde labeling whether the dying cells have actually projected axons out the "incorrect" nerve. In addition, cell death is not used as a correction mechanism in the motor neuron system (Oppenheim, 1981).

Consistent with previous studies (Furber *et al.*, 1987; Landmesser and Pilar, 1974b), we saw a 50% decrease in neuron between St. 33/34 and St. 40, although our cell counts differed. The number of neurons we obtained at St. 33/34 was considerably higher than previous estimates (17,000 prior to cell death versus 6500); however, other studies incorporated a correction factor (Abercrombie,

1946) that could have underestimated the neuronal number. The larger number we found corroborates the higher numbers of St. 33/34 CG neurons recovered in cell culture (Nishi and Berg, 1979; Tuttle *et al.*, 1980). We also found that the absolute number of neurons within the CG differed according to the strain of chicken from which the fertilized eggs were taken. We consistently saw >50% more neurons per CG from the New Hampshire Red × White Leghorn hybrids in comparison to embryos from a pure White Leghorn stock.

It is unclear if the control of cell death at St. 29 is similar to that between St. 33/34 and St. 40. Our experiments revealed that the large amount of cell death at St. 29 was influenced by the environment—target ablation at St. 11–13 (E2) exacerbated cell death and overexpression of chCNTF reduced cell death. These are the hallmarks of target-dependent cell death, yet it is unlikely to be regulated by interactions involving synaptogenesis, since few peripheral synapses have formed at St. 29 (Meriney and Pilar, 1987; Pilar *et al.*, 1987). However, the neurons dying at St. 29 are likely to have extended neurites into the optic cup toward their future target tissues, since Landmesser observed that ciliary and choroid nerves could conduct action potentials as early as St. 25 (Landmesser and Pilar, 1972). Thus, the removal of the optic vesicle at E2 could have disrupted the environment in which CG axons pathfind. For example, GDNF produced by the optic vesicle has been proposed to promote neurite outgrowth (Hashino *et al.*, 2000). Disruption of local GDNF concentrations may have exacerbated cell death. Alternatively, we have shown that St. 29 CG neurons are CNTF-dependent; thus, the developing optic cup may express chCNTF, which is necessary for supporting CG neuron survival. Consistent with this hypothesis, we have observed chCNTF expression in the eye at St. 29 (Finn and Nishi, unpublished results), and overexpressing chCNTF decreased cell death significantly at St. 29. Interestingly, both optic vesicle ablation (Landmesser and Pilar, 1974a) and overexpression of chCNTF (Finn *et al.*, 1998) do not alter the total number of neurons at St. 34, but result in significant changes by St. 40. The latency observed in total neuronal cell number could be due to the compensation for neuronal loss by the precursor population.

In summary, these studies reveal a complex pattern of cell death during CG development and suggest that an internal homeostatic mechanism controls neuron number early in development. This dynamic process of cell death and replacement prior to peripheral synaptogenesis should be taken into consideration in future studies of cell death in the CG. For example, manipulations that exacerbate early cell death could deplete the number of postmitotic precursors, leading to changes in final neuron number in the mature CG. It will be of interest to determine whether similar mechanisms are in operation in other nervous tissues.

ACKNOWLEDGMENTS

We thank Dr. Steven Matsumoto, Gillian Bunker, Midori Seppa, Dr. Jan Christian, and Dr. Felix Eckenstein for their helpful comments on the manuscript. The full-length cDNA encoding chCNTFR α (GPAR α) was obtained from Dr. Hermann Rohrer. pRCASBP(A)-GFP was a kind gift from Dr. Connie Cepko. We are indebted to Dr. Gary Banker and his laboratory for the use of their imaging setup and software. We thank Dr. Michael Marusich and Dr. Jim Weston for their generous gift of anti-HuA. The DF-1 cell line was obtained from Dr. Doug Foster. We also thank Geoff Greene at Microbrightfield for technical advice regarding the use of stereology and Aurelie Snyder for her assistance with the confocal microscope. This study was funded by NS25767 (R.N.) and N. L. Tartar fellowship (V.M.L.).

REFERENCES

- Abercrombie, M. (1946). Estimation of nuclear population from microtome sections. *Anat. Rec.* **94**, 239–247.
- Avivi, C., and Goldstein, R. S. (1999). Differential expression of Islet-1 in neural crest-derived anglia: Islet-1 + dorsal root ganglion cells are post-mitotic and Islet-1 + sympathetic ganglion cells are still cycling. *Brain Res. Dev. Brain Res.* **115**, 89–92.
- Barde, Y.-A. (1989). Trophic factors and neuronal survival. *Neuron* **2**, 1525–1534.
- Barembaum, M., Moreno, T. A., LaBonne, C., Sechrist, J., and Bronner-Fraser, M. (2000). Noelin-1 is a secreted glycoprotein involved in generation of the neural crest. *Nat. Cell Biol.* **2**, 219–225.
- Blaschke, A. J., Staley, K., and Chun, J. (1996). Widespread programmed cell death in proliferative and postmitotic regions of the fetal cerebral cortex. *Development* **122**, 1165–1174.
- Blaschke, A. J., Weiner, J. A., and Chun, J. (1998). Programmed cell death is a universal feature of embryonic and postnatal neuroproliferative regions throughout the central nervous system. *J. Comp. Neurol.* **396**, 39–50.
- Bronner-Fraser, M., and Cohen, A. M. (1980). Analysis of the neural crest ventral pathway using injected tracer cells. *Dev. Biol.* **77**, 130–141.
- Chu-Wang, I. W., and Oppenheim, R. W. (1978). Cell death of motoneurons in the chick embryo spinal cord. II. A quantitative and qualitative analysis of degeneration in the ventral root, including evidence for axon outgrowth and limb innervation prior to cell death. *J. Comp. Neurol.* **177**, 59–85.
- D'Amico-Martel, A. (1982). Temporal patterns of neurogenesis in avian cranial sensory and autonomic ganglia. *Am. J. Anat.* **163**, 351–372.
- Dryer, S. E. (1994). Functional development of the parasympathetic neurons of the avian ciliary ganglion: A classic model system for the study of neuronal differentiation and development. *Prog. Neurobiol.* **43**, 281.
- Dupin, E. (1984). Cell division in the ciliary ganglion of quail embryos *in situ* and after back-transplantation into the neural crest migration pathways of chick embryos. *Dev. Biol.* **105**, 288–299.
- Ellis, H. M., and Horvitz, H. R. (1986). Genetic control of programmed cell death in the nematode *C. elegans*. *Cell* **44**, 817–829.
- Ericson, J., Thor, S., Edlund, T., Jessell, T. M., and Yamada, T. (1992). Early stages of motor neuron differentiation revealed by expression of homeobox gene Islet-1. *Science* **256**, 1555–1560.

- Finn, T. P., Kim, S., and Nishi, R. (1998). Overexpression of ciliary neurotrophic factor in vivo rescues chick ciliary ganglion neurons from cell death. *J. Neurobiol.* **34**, 283–293.
- Finn, T. P., and Nishi, R. (1996). Expression of a chicken ciliary neurotrophic factor in targets of ciliary ganglion neurons during and after the cell death phase. *J. Comp. Neurol.* **366**, 559–571.
- Furber, S., Oppenheim, R. W., and Prevette, D. (1987). Naturally-occurring neuron death in the ciliary ganglion of the chick embryo following removal of preganglionic input: Evidence for the role of afferents in ganglion cell survival. *J. Neurosci.* **7**, 1816–1832.
- Hamburger, V., and Hamilton, H. L. (1951). A series of normal stages in the development of the chick embryo. *J. Morphol.* **88**, 49–92.
- Hamburger, V., and Levi-Montalcini, R. (1949). Proliferation, differentiation, and degeneration in the spinal ganglia of the chick embryo under normal and experimental conditions. *J. Exp. Zool.* **111**, 457–502.
- Hashino, E., Shero, M., Eddins, A. C., Milbrandt, J., and Johnson, E. M. (2000). GDNF and NRTN are target-derived trophic factors essential for ciliary ganglion neuron development. *Soc. Neurosci. Abstr.* **26**, 606.27.
- Heller, S., Finn, T. P., Huber, J., Nishi, R., Geissen, M., Püschel, A. W., and Rohrer, H. (1995). Analysis and expression of the chick GPA receptor suggests multiple functions in neuronal development. *Development* **121**, 2682–2693.
- Himly, M., Foster, D. N., Bottoli, I., Iacovoni, J. S., and Vogt, P. K. (1998). The DF-1 chicken fibroblast cell line: Transformation induced by diverse oncogenes and cell death resulting from infection by avian leukosis viruses. *Virology* **248**, 295–304.
- Homma, S., Yaginuma, H., and Oppenheim, R. W. (1994). Programmed cell death during the earliest stages of spinal cord development in the chick embryo: A possible means of early phenotypic selection. *J. Comp. Neurol.* **345**, 377–395.
- Kuida, K., Haydar, T. F., Kuan, C. Y., Gu, Y., Taya, C., Karasuyama, H., Su, M. S., Rakic, P., and Flavell, R. A. (1998). Reduced apoptosis and cytochrome c-mediated caspase activation in mice lacking caspase 9. *Cell* **94**, 325–337.
- Kuida, K., Zheng, T. S., Na, S., Kuan, C.-Y., Yang, D., Karasuyama, H., Rakic, P., and Flavell, R. A. (1996). Decreased apoptosis in the brain and premature lethality in CPP32-deficient mice. *Nature* **384**, 368–372.
- Landmesser, L., and Pilar, G. (1972). The onset and development of transmission in the chick ciliary ganglion. *J. Physiol.* **222**, 691–713.
- Landmesser, L., and Pilar, G. (1974a). Synapse formation during embryogenesis on ganglion cells lacking a periphery. *J. Physiol.* **241**, 715–736.
- Landmesser, L., and Pilar, G. (1974b). Synaptic transmission and cell death during normal ganglionic development. *J. Physiol.* **241**, 737–749.
- Leung, D. W., Parent, A. S., Cachianes, G., Esch, F., Coulombe, J. N., Nikolics, K., Eckenstein, F. P., and Nishi, R. (1992). Cloning, expression during development, and evidence for secretion of a trophic factor for ciliary ganglion neurons. *Neuron* **8**, 1045–1053.
- Lockshin, R., and Williams, C. (1965). Programmed cell death. II. Endocrine potentiation of the breakdown of the intersegmental muscles of silkworms. *J. Insect Physiol.* **11**, 803–809.
- Marusich, M. F., Furneaux, H. M., Henion, P. D., and Weston, J. A. (1994). Hu neuronal proteins are expressed in proliferating neurogenic cells. *J. Neurobiol.* **25**, 143–155.
- Marwitt, G. R., Pilar, G., and Weakly, J. N. (1971). Characterization of two cell populations in the avian ciliary ganglion. *Brain Res.* **25**, 317–334.
- Meriney, S. D., and Pilar, G. (1987). Cholinergic innervation of the smooth muscle cells in the choroid coat of the chick eye and its development. *J. Neurosci.* **7**, 3827–3839.
- Morgan, B. A., and Fekete, D. M. (1996). Manipulating gene expression with replication-competent retroviruses. *Methods Cell Biol.* **51**, 185–218.
- Narayanan, C. H., and Narayanan, Y. (1978). Neuronal adjustments in developing nuclear centers of the chick embryo following transplantation of an additional optic primordium. *J. Embryol. Exp. Morphol.* **44**, 53–70.
- Nijhawan, D., Honarpour, N., and Wang, X. (2000). Apoptosis in neural development and disease. *Annu. Rev. Neurosci.* **23**, 73–87.
- Nishi, R. (1994). Target-derived molecules that influence the development of neurons in the avian ciliary ganglion. *J. Neurobiol.* **25**, 612–619.
- Nishi, R. (1996). Autonomic and sensory neuron cultures. *Methods Cell Biol.* **51**, 249–263.
- Nishi, R., and Berg, D. K. (1979). Survival and development of ciliary ganglion neurones grown alone in cell culture. *Nature* **277**, 232–234.
- Noden, D. M. (1975). An analysis of migratory behavior of avian cephalic neural crest cells. *Dev. Biol.* **42**, 106–130.
- Oppenheim, R. W. (1981). Cell death of motoneurons in the chick embryo spinal cord. V. Evidence on the role of cell death and neuromuscular function in the formation of specific peripheral connections. *J. Neurosci.* **1**, 141–151.
- Oppenheim, R. W. (1991). Cell death during development of the nervous system. *Annu. Rev. Neurosci.* **14**, 453–501.
- Pilar, G., Landmesser, L., and Burstein, L. (1980). Competition for survival among developing ciliary ganglion cells. *J. Neurophysiol.* **43**, 233–254.
- Pilar, G., Nunez, R., McLennan, I. S., and Meriney, S. D. (1987). Muscarinic and nicotinic synaptic activation of the developing chicken iris. *J. Neurosci.* **7**, 3813–3826.
- Rohrer, H., and Sommer, I. (1983). Simultaneous expression of neuronal and glial properties by chick ciliary ganglion cells during development. *J. Neurosci.* **3**, 1683–1693.
- Rohrer, H., and Thoenen, H. (1987). Relationship between differentiation and terminal mitosis: Chick sensory and ciliary neurons differentiate after terminal mitosis of precursor cells, whereas sympathetic neurons continue to divide after differentiation. *J. Neurosci.* **7**, 3739–3748.
- Sechrist, J. W., Wolf, J., and Bronner-Fraser, M. (1998). Age-dependent neurotransmitter plasticity of ciliary ganglion neurons. *Mol. Cell. Neurosci.* **12**, 311–323.
- Shah, N. M., and Anderson, D. J. (1997). Integration of multiple instructive cues by neural crest stem cells reveals cell-intrinsic biases in relative growth factor responsiveness. *Proc. Natl. Acad. Sci. USA* **94**, 11369–11374.
- Tsuhida, T., Ensini, M., Morton, S. B., Baldassare, M., Edlund, T., Jessell, T. M., and Pfaff, S. L. (1994). Topographic organization of embryonic motor neurons defined by expression of LIM homeobox genes. *Cell* **79**, 957–970.
- Tuttle, J. B., Suszkiw, J. B., and Ard, M. (1980). Long-term survival and development of dissociated parasympathetic neurons in culture. *Brain Res.* **183**, 161–180.

- Vaux, D. L., and Korsmeyer, S. J. (1999). Cell death in development. *Cell* **96**, 245–254.
- Wakamatsu, Y., and Weston, J. A. (1997). Sequential expression and role of Hu RNA-binding proteins during neurogenesis. *Development* **124**, 3449–3460.
- Wakamatsu, Y., Mochii, M., Vogel, K. S., and Weston, J. A. (1998). Avian neural crest-derived neurogenic precursors undergo apoptosis on the lateral migration pathway. *Development* **125**, 4205–4213.
- West, M. J., Slomianka, L., and Gundersen, H. J. G. (1991). Unbiased stereological estimation of the total number of neurons in the subdivisions of the rat hippocampus using the Optical Fractionator. *Anat. Rec.* **231**, 482–497.

Received for publication December 1, 2000

Revised January 31, 2001

Accepted February 16, 2001

Published online April 16, 2001